

Electrochemical Biosensor Based on Nicotinamide Adenine Dinucleotide/Gold Nanoparticles Composite for Determination of the Antioxidant Activity of Caffeic Acid

Emad F. Newair¹, Refat Abdel-Hamid^{1,*} and Ayman Nafady^{1,2}

¹ Unit of Electrochemistry Applications (UEA), Department of Chemistry, Faculty of Science, University of Sohag, Sohag 82524, Egypt

² Department of Chemistry, College of Science, King Saud University, Riyadh, Saudi Arabia

Received: 19 Jul. 2017, Revised: 22 Aug. 2017, Accepted: 28 Aug. 2017.

Published online: 1 Sep. 2017.

Abstract: As a consequence of normal aerobic metabolism, reactive oxygen species (ROS) are produced and induce DNA oxidative damage. The evaluation of the protective effect of antioxidant caffeic acid (CAF) was achieved by examining the integrity of the DNA nucleobases using square wave voltammetry (SWV). Herein, an electrochemical biosensor based on nicotinamide adenine dinucleotide (NADH) was used for the assessment of the antioxidant activity. The biosensor was constructed via successive voltammetric scanning of a 0.9 μM NADH solution using glassy carbon electrode modified with gold nanoparticles (AuNPs/GCE) in 0.2 M phosphate-buffer saline (PBS) at room temperature. The method was based on the partial damage of a NADH layer adsorbed on the electrode surface by $\text{OH}\cdot$ radicals generated by Fenton reaction. Upon immersion of the sensor in Fenton solution mixture, current response is decreased due to competitive interaction between NADH with the hydroxyl radicals and the direct oxidation of NADH on the electrode. On addition of CAF, the oxidation response is increased. This is attributed to the scavenging of the hydroxyl radicals by CAF leaving more adenines unoxidized, and thus, increasing the electrocatalytic current of NADH. The caffeic acid scavenging percentage to $\cdot\text{OH}$ was evaluated. The results show that the scavenging potency of CAF is best at 50.0 μM and calculated to be 66.92 %.

Keywords: Caffeic acid, NADH, Antioxidant activity, Square wave voltammetry, Biosensor

1 Introduction

Caffeic acid (CAF) is one of the most abundant derivatives of cinnamic acids and found naturally in a wide variety of materials derived from plants such as wine, coffee beans, fruits, vegetables, olive oil and tea [1]. It exhibits a wide variety of physiological activity as antioxidant, anti mutagenic and anti carcinogenic [2]. CAF is considered to be an important part of the general plant defense mechanism against infection predation [3].

Natural polyphenol antioxidants are interesting compounds, including caffeic acid (CAF), which have protective activity against oxidative damages in vitro relating to various diseases such as cancer, cardiovascular diseases, and diabetes [4-7]. Several methods such as spectrophotometric, electroanalytical and Ems methods were utilized to measure the antioxidant activity of various compounds. In this context, CAF antioxidant activity was early evaluated

spectrophotometrically using 2,2-diphenyl-1-picrylhydrazyl (DPPH) [8].

Construction of electrochemical sensors and/or biosensors using nano structured materials has attracted great attention and the past few decades have witnessed enormous interest in biological and chemical sensors based on metal nano particles, particularly gold nano particles (Au NPs) owing to their interesting physicochemical properties [10]. Of particular relevance to the present study, Neto et al. [11], have shown that AuNPs supported on MWCNTs displayed very strong catalytic behavior towards dihydronicotinamide adenine dinucleotide (NADH) oxidation [12-16]. In these studies, the antioxidant assessment is carried out via NADH-based biosensors. The activity of antioxidant in biological systems associated with the sensor response is principally related to mimicking the damage caused in vivo by reactive oxygen species (ROS) [17]. In this scenario, the biosensor is constructed via immobilization of NADH onto glassy carbon electrodes (GCE), by adsorptive processes, and then exposed to ROS and antioxidant compounds. The response of

*Corresponding author E-mail: refat.abdelhamid@science.sohag.edu.eg

electrochemical NADH is usually probed by square wave voltammetry (SWV) whereas the damage of NADH (induced by ROS) is estimated by analyzing the decrease in the corresponding oxidation current. On the other hand, the antioxidant protective effect promoted on the sensor can be estimated by observing the electrochemical current increase attributed to the scavenging activity of the antioxidant.

In the present investigation, we have developed a biosensor comprising dihydronicotinamide adenine dinucleotide/gold nanoparticles/glassy carbon electrode, NADH/AuNPs/GCE, for the determination of the antioxidant activity of caffeic acid (CAF) in 0.2 M phosphate-buffer solution. The voltammetric method is used to assess the OH• radical scavenging abilities of CAF acid. After immersion of the sensor in the Fenton mixture, the generated oxidative products are indirectly quantified after measuring the remained unoxidized NADH on the electrode surface. The increase in the electrocatalytic current in the presence of the antioxidant species is thus monitored.

2 Experimental

2.1 Reagents

All the chemicals, caffeic acid (CAF), dihydronicotinamide adenine dinucleotide (NADH) and gold nano-particles (5 nm) were purchased from Sigma. Disodium hydrogen phosphate, sodium dihydrogen phosphate, phosphoric acid and sodium hydroxide (A R chemicals, Merck) are used without further purifications.

2.2 Preparation of Solutions

A fresh 0.2 M phosphate buffer solutions (PBS) supporting electrolyte with different pH values were prepared from monosodium phosphate and disodium phosphate in deionized water. Phosphoric acid was used to adjust pH values. From dry pure substances, fresh stock standard solutions (10 mM) were prepared in the PBS. The working solutions were diluted to the convenient concentration just prior to use.

Fenton solution mixture (for generation of hydroxyl radicals) was prepared by mixing Fe²⁺:EDTA: H₂O₂ (in the molar ratio of 1:2:40) μM. Mello et al reported that when an excess of hydrogen peroxide was added in the reaction medium, a high NADH damage was observed [18].

2.3 Electrochemistry

Cyclic (CV) and square sweep (SWV) voltammetric measurements were undertaken on Auto lab PGSTAT128N

Potentiostat/Galvanostat (Eco-Chemie, Utrecht, Netherlands) coupled with a NOVA 2.0 software. A standard three-electrode electrochemical cell equipped with bare and modified glassy carbon electrode as working electrode (GCE, diameter = 3.0 mm, model 61204300, Metrohm-Autolab, Switzerland), silver/silver chloride (Ag/AgCl, aq. KCl, 3.0 M) as a reference electrode, and a platinum wire is used as auxiliary electrode. A pH- 213 Microprocessor pH Meter from HANNA instruments was used to measure the pH of desired solutions.

2.4 Immobilization of Dihydronicotinamide Adenine Dinucleotide (NADH) onto Gold Nano particles-Modified Glassy Carbon Electrode (Au NPs/GCE).

Glassy carbon working electrode was polished successively with 0.5 μm alumina powder on a polishing cloth. After rinsing the surface thoroughly with deionized water, the polished GCE was sonicated for 5 min in water/ethanol and rinsed again with water, and then the surface was fully dried at atmospheric condition. 10 μL of the suspended gold colloid (5 nm) was dropped onto the clean GCE surface to construct AuNPs/GCE and then the solvent was evaporated over night. The modified GCE, NADH/Au NPs/GCE, was fabricated by voltammetric cycling (one cycle) over the potential range from 0 to 0.6 V Vs Ag/AgCl in 0.2 M PBS (pH 5.18) containing 0.9 μM NADH using scan rate of 100 mV s⁻¹. The fabrication procedures involve four steps: (a) immobilization of AuNPs and NADH onto GCE surface; (b) damage of NADH by the immersion of the NADH/AuNPs/GCE in a freshly prepared Fenton mixture; (c) study the influence of the antioxidant (caffeic acid) on the system; (d) electro-oxidation of the remaining un-oxidized NADH. Finally, after exposure for a fixed time intervals (reaction time), the biosensor electrode was washed with water and immediately immersed in a 0.2 M PBS (pH 5.18) to carry out the electro-oxidation of the remaining un-oxidized base.

2.5 Evaluation of the Biosensor Performance

After exposing the NADH/AuNPs/GCE to the Fenton mixture in the presence (I_a) and the absence (I_d) of a fixed amount of caffeic acid, the electrocatalytic current obtained was selected as a criteria for optimization. I_d is the minimum electrocatalytic current value under each experimental condition since the absence of the antioxidant in the damaging solution precludes the protection of the NADH from radical oxidation, thereby leaving the lowest amount of the base for further electrochemical oxidation.

Thus, the ratio of maximum value will be selected in each optimization.

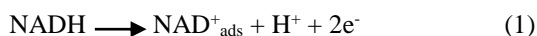
3 Results and Discussion

3.1 Electrochemical Behavior of NADH on AuNPs/GCE

Fig.1 contains cyclic voltammograms (CV) obtained at scan rate of 20 mV s^{-1} using AuNPs / GCE in the absence and the presence of $0.9 \mu\text{M}$ NADH in 0.2 M PBS, pH 5.18. Apparently, in the absence of NADH, the electrode did not show any electrochemical activity over the potential range (0 to 0.6 V) of study, thereby indicating that the modified AuNPs/GCE is electro-inactive with no detection of any gold oxidation wave. In a marked contrast, in the presence of NADH, an irreversible oxidation wave with high catalytic current is observed with a peak potential (E_p^a) of 0.38 V. This irreversible response, even at faster scan rates, is indicative of a totally-irreversible oxidation of the NADH, caused by a fast follow-up chemical reaction [19]. This irreversible behavior was also observed even when a bare GCE is used for direct electrochemical oxidation of NADH to the cationic species NAD^+ but under these conditions, it occurs at markedly higher oxidation over potential $E_p^a > 0.85 \text{ V}$. Moreover, as shown in previous work, the oxidation process is quite complicated and accompanied by an electrode fouling problems that arise from generation of polymeric side products along with the strong adsorption of the oxidized product (NAD^+) at electrode surface [15,20]. Indeed, these problems were overcome by using modified AuNPs/GCE. In view of this finding we concluded that modification of GCE with AuNPs enhances its electrochemical sensitivity towards NADH and eliminates or minimizes the adsorption problems associated with the generated products.

3.2 Effect of Ph

Samec and Elving reported the electrochemical oxidation of NADH at gold and platinum electrodes at various pH values and NADH concentrations. They concluded that the oxidation process occurs via a single two-electron step to generate the enzymatically active NAD^+ product [20] (Eq 1).



The electrocatalytic oxidation current response of $0.9 \mu\text{M}$ NADH in 0.2 M PBS at different pH values (1.6 to 9.13) was investigated on AuNPs/GCE by cyclic voltammetry at scan rate of 100 mV s^{-1} . As can be seen in Fig 2, the oxidation peak potential, E_p^a , is a nodically shifted upon increasing the solution pH. The E_p^a - pH relationship

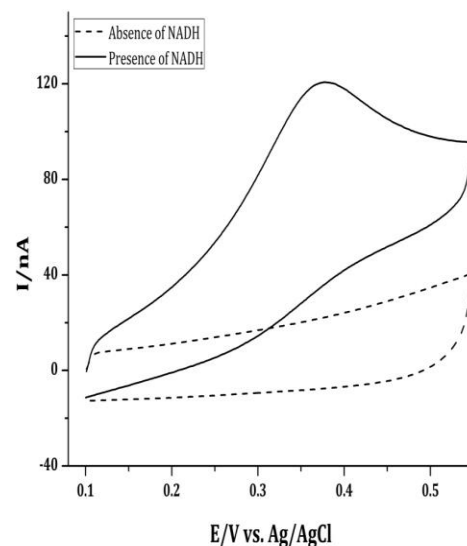


Fig 1. Cyclic Voltammograms obtained with AuNPs/GCE in the absence (dotted line) and the presence (solid line) of $0.9 \mu\text{M}$ NADH in 0.2 M PBS, pH 5.18 using scan rate of 20 mV s^{-1} .

Was constructed and depicted in Fig.3A. A linear shift of E_p^a towards less positive potentials with increasing pH indicates that protons are directly involved in the oxidation of NADH. The overall behavior is represented by Eq 2.

$$E_p(\text{V}) = 0.522 - 0.0231\text{pH} \quad r = 0.953 \quad (2)$$

Virtually, the obtained slope of -23.1 mV/pH is relatively close from the Nernstian value of -29.5 mV for a two-electron, one-proton, process at 25°C [21]. Importantly, as can be seen in Fig. 3B, the oxidation peak current, i_p^a , does not follow a particular trend upon increasing the pH of solution from acidic to basic. However, the highest anodic peak current is obtained at pH 6.5, thus a pH value of 5.18 was chosen for the construction of NADH sensor, and the subsequent experiments.

3.3 Effect of Scan Rate

Cyclic voltammograms obtained for $0.9 \mu\text{M}$ NADH in 0.2 M PBS (pH 5.18) at different scan rates (5.0 to 300 mV s^{-1}) using AuNPs/GCE are shown in Fig.4A. Clearly, highly irreversible oxidation wave is observed at all scan rates, thereby indicating that the follow up reaction is extremely fast and cannot be outrun by higher scan rates up to 500 mV s^{-1} . Analysis of the extracted parameters from this scan rate study reveals that the oxidation peak current (i_p^a) increased linearly with scan rates over the entire range (5 to 300 mV s^{-1}). Moreover, a linear $\log - \log$

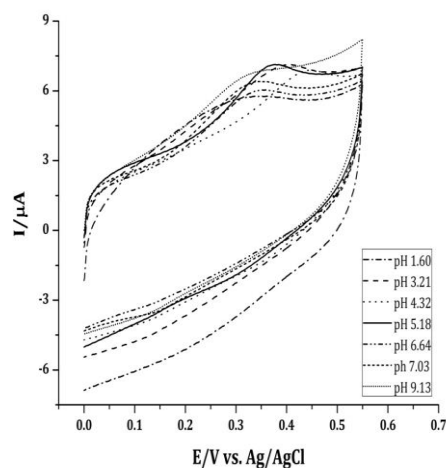


Fig 2. Cyclic voltammograms of 0.9 μM NADH on AuNps/GCE in 0.2 M PBS with different pH's at scan rate of 100 mV s^{-1} .

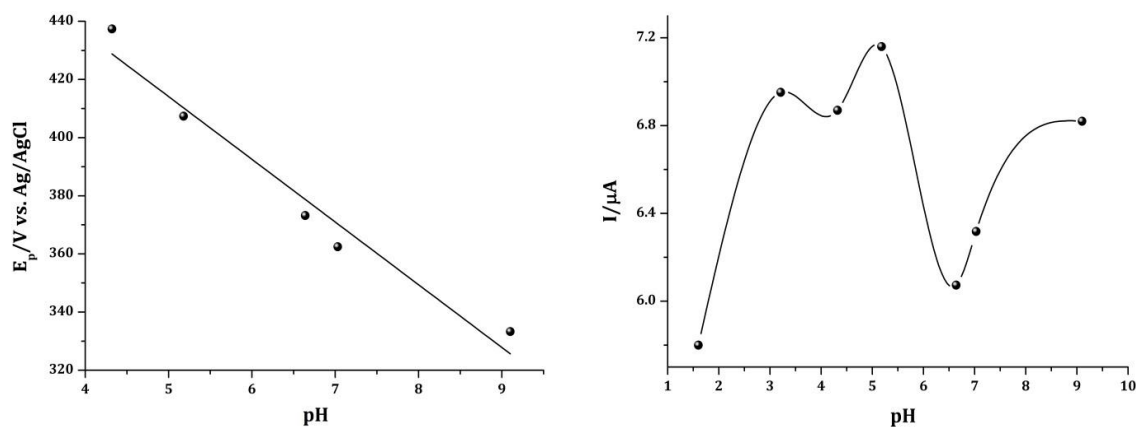


Fig 3. Effects of pH of 0.9 μM NADH at AuNPs/GCE in 0.2 M PBS under different pH: 1.6, 3.21, 4.32, 5.18, 6.64, 7.03, 9.1 on the oxidation potential (A); and oxidation current (B).

variation ($\log i_p^a$ versus $\log v$) for the oxidation wave is obtained with slope of 0.89, as illustrated in Fig.4B. This behavior suggests that the electrochemical oxidation response of NADH on the modified electrode was an adsorption-controlled process [22].

3.4 Effect of Concentration

Fig.5A represents the effect of NADH concentration on the voltammetric response in aqueous 0.2 M PBS (pH 5.18) using AuNPs/GCE and scan rate of 100 mV s^{-1} . Over the concentration range of investigation ($1.6 - 8.21 \times 10^{-4}$ M)

only one irreversible oxidation wave is obtained. As shown in Fig. 5A, the magnitude of the oxidation peak current (i_{pa}) depends on the concentration of NADH. Interestingly, plotting of i_{pa} values versus [NDAH] (Fig. 5B) revealed that, i_{pa} is linearly increased with increasing NADH concentrations up to 5.5×10^{-4} M. Upon further increase of concentration, the response tends to levels off. This behavior indicates that NADH is adsorbed at electrode surface, and at concentration $>5.5 \times 10^{-4}$ M the electrode surface seems to be completely covered.

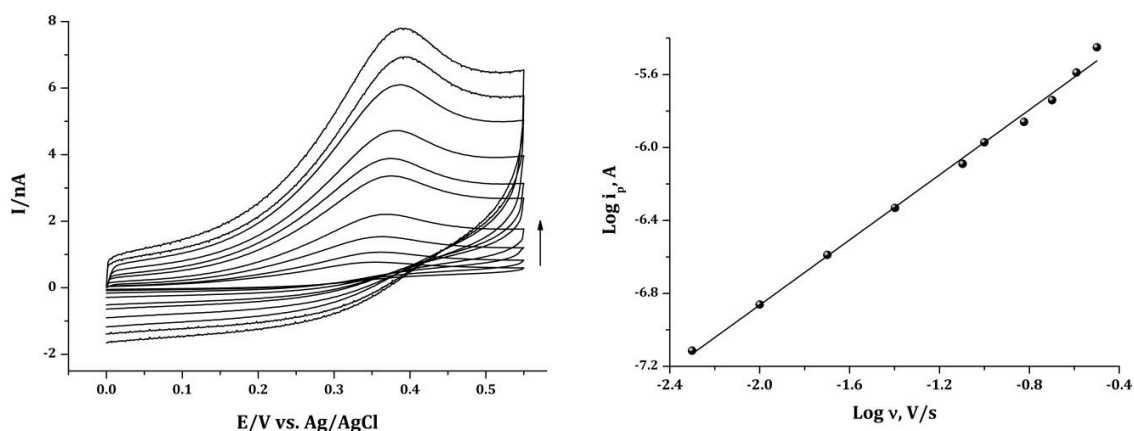


Fig 4. (A) Cyclic Voltammograms of 0.9 μM NADH obtained with AuNPs/GCE in 0.2 M PBS, pH 5.18, at different scan rates (5, 10, 20, 40, 80, 100, 150, 200, 250 and 300 mV s^{-1}); (B) Plot of log anodic peak current (i_p^a) versus log scan rate (v).

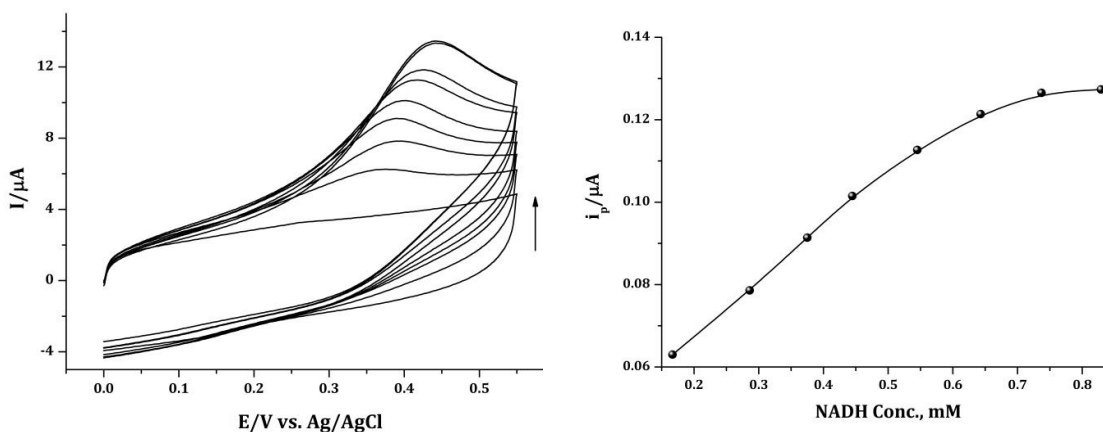


Fig 5. (A) Cyclic voltammograms obtained at scan rate of 100 mV s^{-1} for NADH using AuNPs/GCE in 0.2 M PBS, pH 5.18 as a function of NADH concentrations; (B) Dependence of the voltammetric peak current, i_p^a , on NADH concentration.

3.5 Construction of Electrochemical NADH Biosensor

The electrochemical biosensor, AuNPs/GCE-NADH, was constructed via successive voltammetric cycling of the potential over the range (0 to 0.6 V) for 0.9 μM NADH solution on AuNPs/GCE in 0.2 M PBS (pH 5.18) at scan rate of 100 mV s^{-1} (Fig. 6). Apparently, the first cycle has a markedly higher oxidative current compare to second one and continue to decrease with increasing the number of cycles (20 cycles shown). This behavior is attributed to the adsorption of a small amount of NAD^+ that was produced during the first CV scan. At the consecutive cycles, the amount of the adsorbed species is increased and consequently the active area of the electrode that is exposed

to substrate is diminished. This extensive coverage of the electrode with increasing the number of cycles is the reason for the massive decrease in current.

3.6 Evaluation of Hydroxyl Radical Scavenging Activities of Caffeic Acid

Given that square sweep Voltammetry (SWV) is a highly sensitive technique compared to CV, it is commonly utilized for monitoring and detecting the response of antioxidant activities. Fig.7 shows the SW voltammograms of AuNPs/GCE biosensor before and after interaction with Fenton solution. Curve 1 represents the modified electrode response when it is directly immersed in phosphate buffer, whereas curves 2 and 3 are obtained upon

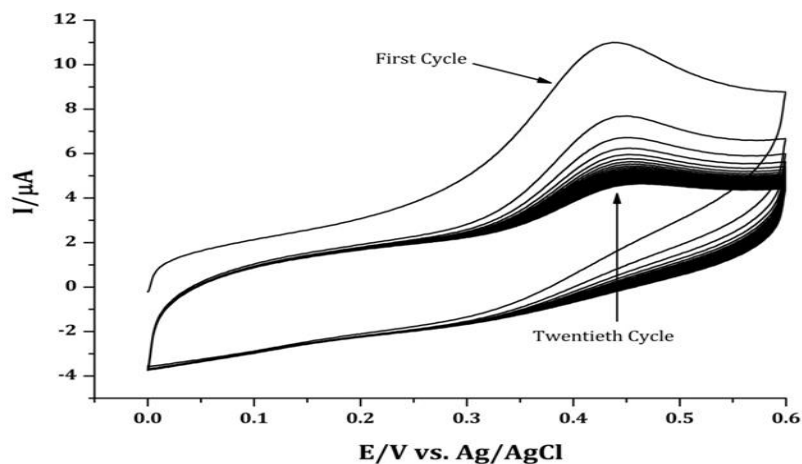


Fig 6. Cyclic voltammograms showing the effect of multi cycles of $0.9 \mu\text{M}$ NADH on AuNPs/GCE in 0.2 M PBS, pH 5.18, and scan rate of 100 mV s^{-1} .

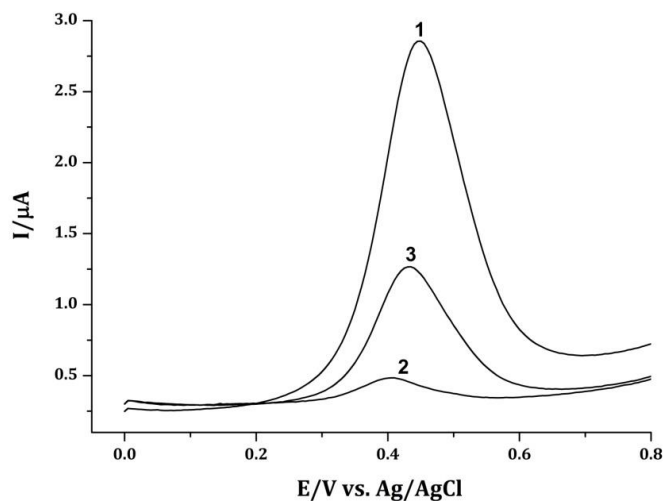


Fig 7. SWV curves of the NADH/AuNPs/GCE biosensor obtained in 0.2 M PBS, pH 4.35. Potential range from +0.0 to +0.8 V, frequency=40 Hz, $E_{\text{step}}=15 \text{ mV}$, $E_{\text{amplitude}}=15 \text{ mV}$: (1) NADH-based biosensor signal (blank); (2) NADH-based biosensor signal after immersion in the Fenton solution: Fe^{2+} : EDTA: H_2O_2 (1:2:20); (3) NADH-based biosensor signal after immersion in the Fenton solution containing $50.10 \mu\text{M}$ CAF. Immersion time of the electrode in the Fenton solution is 30 s.

immersion of the biosensor in Fenton solution mixture (curve2) and CAF(curve3) respectively. Apparently, the high oxidation current observed in PBs solution only is drastically decreased upon exposure of the modified electrode to Fenton mixture, owing to competitive interaction of NADH with hydroxyl radicals, generated by the Fenton system, and the direct oxidation of NADH on the electrode surface. However, upon addition of CAF, the oxidation current is increased again. This response is attributed to the scavenging of the hydroxyl radicals by CAF. It was known that CAF has strongly polar hydroxyl groups, which is closely related to its antioxidant action[6].

In view of the above finding, the effect of caffeic acid(CAF) antioxidant protection on the NADH based sensor can be estimated by observing the increase in the electrochemical current attributed to the scavenging activity [6]. This is undertaken by probing the dependence of the scavenging percentage of $\cdot\text{OH}$ radicals on CAF

concentration. Thus, upon increasing the concentration of CAF, an increase of the scavenging percentage is observed. As shown in Fig.8, the antioxidant potency of CAF is very effective over the concentration range from 10.0 to 50.0 μM . Significantly, the scavenging percentage, expressed as the percentage of the electrocatalytic current signal decrease, was calculated for each concentration according to the equation 3:

$$\text{Scavenging Percentage (\%)} = \frac{[I_p - I_a]}{[I_{blank} - I_a]} \times 100 \quad (3)$$

Where I_{blank} is the peak current recorded in PBS as a blank signal, I_p and I_a are the peak current in presence and absence of CAF, respectively. The results show that the scavenging potency of CAF for $\cdot\text{OH}$ is highest at 50.0 μM CAF and calculated to be 66.92 %.

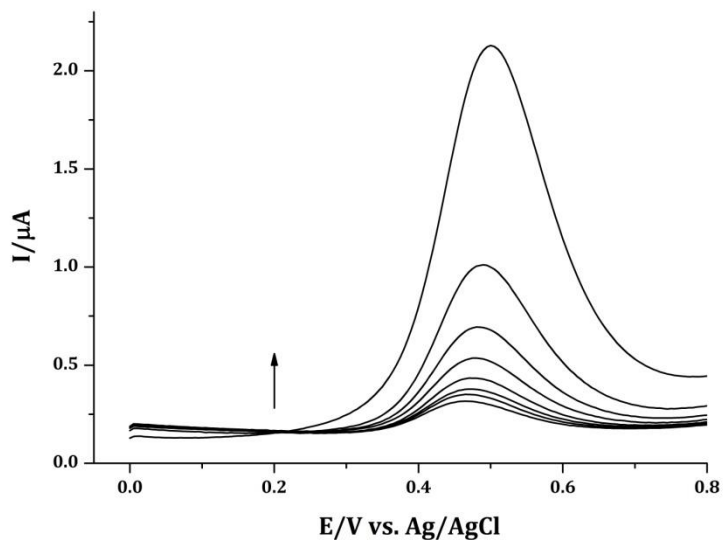


Fig. 8: SWV curves of the NADH/AuNPs/GCE biosensor obtained in 0.2 M PBS, pH 4.35(OR 5.18), after immersion in the Fenton solution: Fe^{2+} : EDTA: H_2O_2 (1:2:20) containing different CAF concentrations (PUT CONCENTRATIONS HERE). Immersion time of the electrode in the Fenton solution is 30 s, SWV parameters as above.

Acknowledgement

The authors gratefully acknowledge the financial support given from the Science and Technology Development Fund (STDF), Egypt, Grant No. (5361). We would like also to extend our sincere appreciation to the Deanship of Scientific Research at King Saud University for funding this Research group NO.(RG#236).

References

- [1] Bassil, D.; Makris, D. P.; Kefalas, P. *Food Res. Int.* 38 (2005) 395.
- [2] Santos, D. P.; Bergamini, M. F.; Fogg, A. G.; Valnice; Zanoni, B., *Microchim. Acta* 151 (2005) 127.
- [3] Moghaddam, A. B.; Ganjali, M. R.; Dinarvand, R.; Norouzi, P.; Saboury, A. A.; Moosavi-Movahedi, A. A., *Biophys. Chem.* 128 (2007) 30.
- [4] Lodovici, M.; Guglielmi, F.; Meoni, M.; Dolara, P., *Food Chem. Toxicol.* 39 (2001) 1205.
- [5] Iwahashi, H.; Ishii, T.; Sugata, R.; Kido, R., *Arch. Biochem. Biophys.* 276 (1990) 242.
- [6] Barroso, M. F.; Noronha, J. P.; Delerue-Matos, C.; Oliveira, M. B. P. P., *J. Agric. Food Chem.* 59 (2011) 5062.
- [7] Rice-Evans, C. A.; Miller, N. J.; Paganga, G., *Trends Plant Sci.* 2 (1997) 152.
- [8] Gaspar, A.; Martins Silva, M. P.; Garrido, E. M.; Garrido, J.; Firuzi, O.; Miri, R.; Saso, L.; Borges, F., *J. Agric. Food Chem.* 58 (2010) 11273.
- [9] Pinczewska, A.; Sosna, M.; Bloodworth, S.; Kilburn, J. D.; Bartlett, P. N., *J. Am. Chem. Soc.* 134 (2012) 18022.
- [10] Parab, H. J.; Chen, Lai T.-C.; Huang, J. H.; Chen, P. H.; Liu, R.-S.; Hsiao, M.; Chen, C.-H.; Tsai, D.-P.; Hwu, Y.-K., *J. Phys. Chem. C.* 113 (2009) 7574.
- [11] Neto, S. A.; Almeida, T. S.; Palma, L. M.; Minteer, S. D.; de Andrade, A. R., *J. Power Sources* 259 (2014) 25.
- [12] Jans, H.; Huo, Q., *Chem. Soc. Rev.* 41 (2012) 2849.
- [13] Liu, Y.; Yuan, R.; Chai, Y.; Tang, D.; Dai, J.; Zhong, X., *Sens. Actuators B*, 115 (2006) 109.
- [14] Quiet, H.; Xue, L.; Ji, G.; Zhou, G.; Huang, X.; Qu, Y. Gao, P., *Biosens. Bioelectron.*, 24 (2009) 3014.
- [15] Radoi, A.; Compagnone, D., *Bioelectrochem.*, 76 (2009) 126.
- [16] Bartlett, P. N.; Simon, E.; Toh, C. S., *Bioelectrochem.*, 56 (2002) 117.
- [17] Barroso, F.; de-los-Santos-Alvarez, N.; Delerue-Matos, C.; Oliveira, M. B. P. P., *Biosens. Bioelectron.*, 30 (2011) 30.
- [18] Mello, L. D.; Hernandez, S.; Marrazza, G.; Mascini, M.; Kubota, L. T., *Biosens. Bioelectron.*, 21 (2006) 1374.
- [19] Rajaram, R. S.; Anandhakumar, S.; Mathiyarasu, J., *J. Electroanal. Chem.*, 746 (2015) 75.
- [20] Samec, Z.; Elving, P. J., *J. Electroanal. Chem.*, 144 (1983) 217.
- [21] Chen, J.; Bao, J.; Cai, C.; Lu, T., *Anal. Chim. Acta*, 516 (2004) 29.
- [22] Bard, A. J.; Faulkner, L. R., *Electrochemical Methods, Fundamentals and Applications*, 2nd ed., 2001, Wiley, New York.